Published by Institute of Physics Publishing for SISSA/ISAS
Received: *September 23, 2002*
Revised: *July 3, 2003*
Accepted: *August 14, 2003*

Shifts in the properties of the Higgs boson from radion mixing*

JoAnne L. Hewett and Thomas Gerard Rizzo

Stanford Linear Accelerator Center, Stanford University
Stanford CA 94309, USA
E-mail: rizzo@slac.stanford.edu, rizzo@slac.stanford.edu

Abstract: We examine how mixing between the Standard Model Higgs boson, h, and the radion present in the Randall-Sundrum model of localized gravity modifies the expected properties of the Higgs boson. In particular, we demonstrate that the total and partial decay widths of the Higgs, as well as the $h \to gg$ branching fraction, can be substantially altered from their Standard Model expectations. The remaining branching fractions are modified less than $\lesssim 5\%$ for most of the parameter space volume.

Keywords: Extra Large Dimensions, Beyond Standard Model, Higgs Physics.

*Work supported by the Department of Energy, Contract DE-AC03-76SF00515.

JHEP08(2003)028

The Randall-Sundrum (RS) model of localized gravity [1] offers a potential solution to the hierarchy problem that can be tested at present and future accelerators [2]. In the original version of this model, the Standard Model (SM) fields are confined to one of two branes that are embedded in a 5-dimensional anti-de Sitter space (AdS_5) described by the metric $ds^2 = e^{-2k|y|}\eta_{\mu\nu}dx^\mu dx^\nu - dy^2$, with $y = r_c\phi$ where r_c is the compactification radius and ϕ describes the 5^{th} dimension. The parameter k characterizes the curvature of the 5-dimensional space and is naturally of order the Planck scale. The two branes form the boundaries of the AdS_5 slice and gravity is localized on the brane located at $y = 0$. Mass parameters on the Standard Model brane, located at $y = r_c\pi$, are red-shifted compared to those on the $y = 0$ brane and are given by $\Lambda_\pi = \overline{M}_{Pl}e^{-kr_c\pi}$, where $\overline{M}_{Pl}$ is the reduced Planck scale. In order to address the hierarchy problem, $\Lambda_\pi \sim$ TeV and hence the separation between the two branes, r_c, must have a value of $kr_c \sim 11-12$. A number of authors [3] have demonstrated that this quantity can be naturally stabilized by a mechanism which leads directly to the existence of a massive bulk scalar field.

Fluctuations about the stabilized RS configuration allow for two massless excitations described in the metric by $\eta_{\mu\nu} \to g_{\mu\nu}(x)$ and $r_c \to T(x)$. The first corresponds to the graviton and $T(x)$ is a new scalar field arising from the g_{55} component of the metric and is known as the radion (r_0). This scalar field corresponds to a quantum excitation of the separation between the two branes. The mass of the radion is proportional to the backreaction of the bulk scalar vacuum expectation value (vev) on the metric. Generally, one expects that the radion mass should be in the range of a few $\times 10\,\text{GeV} \leq m_{r_0} \leq \Lambda_\pi$, where the lower limit arises from radiative corrections and the upper bound is the cutoff of the effective field theory. The radion mass m_{r_0} is then expected to be below the scale Λ_π implying that the radion may be the lightest new field present in the RS model. The radion couples to fields on the Standard Model brane via the trace of the stress-energy tensor with a strength $\Lambda \propto \Lambda_\pi$ of order the TeV scale,

$$\mathcal{L}_{\text{eff}} = -\frac{r_0(x)\,T^\mu_\mu}{\Lambda}\,. \tag{1}$$

Note that $\Lambda = \sqrt{3}\Lambda_\pi$ in the notation of ref. [2]. This leads to gauge and matter couplings for the radion that are qualitatively similar to those of the SM Higgs boson. The collider production and decay of the RS radion has been examined by a number of authors [4, 5] and has been recently reviewed by Kribs [6].

On general grounds of covariance, the radion may mix with the SM Higgs field, which is constrained to the TeV brane, through an interaction term of the form

$$S_{rH} = -\xi \int d^4x\sqrt{-g_{\text{ind}}}R^{(4)}[g_{\text{ind}}]H^\dagger H\,. \tag{2}$$

Here H is the Higgs doublet field, $R^{(4)}[g_{\text{ind}}]$ is the 4-d Ricci scalar constructed out of the induced metric g_{ind} on the SM brane, and ξ is a dimensionless mixing parameter assumed to be of order unity and with unknown sign. The above action induces kinetic mixing between the r_0 and h_0 fields. The resulting lagrangian can be diagonalized by a set of field

JHEP08(2003)028

redefinitions and rotations [7],

$$\begin{aligned} h_0 &= Ah + Br\,, \\ r_0 &= Ch + Dr\,, \end{aligned} \tag{3}$$

with

$$\begin{aligned} A &= \cos\theta - \frac{6\xi\gamma}{Z\sin\theta}\,, \\ B &= \sin\theta + \frac{6\xi\gamma}{Z\cos\theta}\,, \\ C &= -\frac{\sin\theta}{Z}\,, \\ D &= \frac{\cos\theta}{Z}\,, \end{aligned} \tag{4}$$

where h, r represent the physical fields, and

$$\begin{aligned} \gamma &= \frac{v}{\Lambda}\,, \\ Z^2 &= 1 + 6\xi(1-6\xi)\gamma^2\,, \end{aligned} \tag{5}$$

with $v \simeq 246\,\mathrm{GeV}$ being the SM vacuum expectation value. The factor Z serves to bring the physical radion kinetic term to canonical form and as such it must satisfy $Z > 0$. For a fixed value of γ this implies that the range of ξ is bounded, i.e., $\xi_- \leq \xi \leq \xi_+$, where

$$\xi_\pm = \frac{1}{12}\left[1 \pm \left(1 + \frac{4}{\gamma^2}\right)^{1/2}\right], \tag{6}$$

For example, if γ takes on the natural values $\gamma = 0.2(0.1)$ then ξ must lie in the approximate range $-0.754 \leq \xi \leq 0.921(-1.585 \leq \xi \leq 1.752)$. The masses of the physical states, r, h, are then given by

$$m_\pm^2 = \frac{1}{2}\left[T \pm \sqrt{T^2 - 4F}\right], \tag{7}$$

where $m_+(m_-)$ is the larger(smaller) of the two masses and

$$\begin{aligned} T &= (1+t^2)m_{h_0}^2 + \frac{m_{r_0}^2}{Z}\,, \\ F &= \frac{m_{h_0}^2 m_{r_0}^2}{Z^2}\,, \end{aligned} \tag{8}$$

with m_{h_0,r_0} being the weak interaction eigenstate masses and $t = 6\xi\gamma/Z$. This mixing will clearly affect the phenomenology of both the radion and Higgs fields. In particular, the bounds on the Higgs mass from the standard global fit to precision electroweak data are modified, allowing for a Higgs boson (and radion) mass of order several hundred GeV [7]. Here, we examine the modifications to the properties of the Higgs boson, in particular its decay widths and branching fractions, induced by this mixing and find that substantial differences from the SM expectations can be obtained.

JHEP08(2003)028

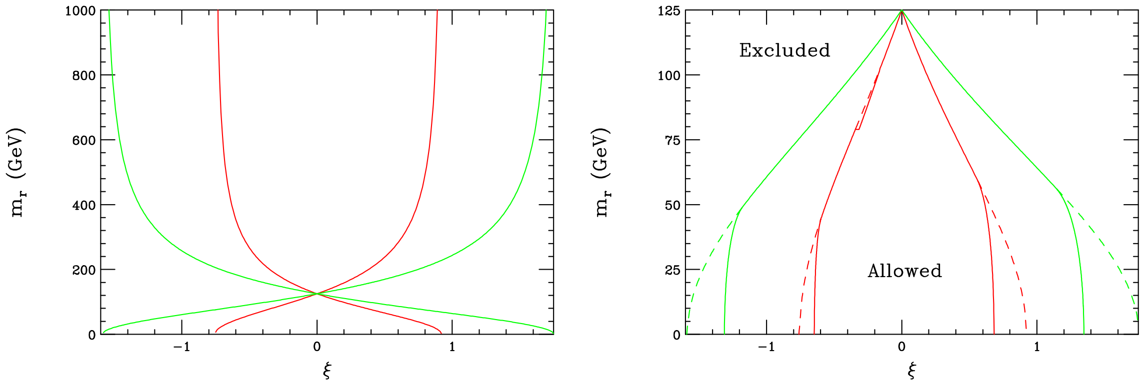

Figure 1: Constraints on the mass of the radion assuming $m_h = 125\,\mathrm{GeV}$ as a function of ξ as described in the text for $\gamma = 0.1$ (green, outer curves) and 0.2 (red, inner curves). The allowed region lies between the solid curves. In the lower panel the regions excluded by LEP searches are also shown and they lie between the corresponding solid and dashed curves.

To make predictions in this scenario we need to specify four parameters: the masses of the physical Higgs and radion fields, $m_{h,r}$, the mixing parameter ξ, and the ratio $\gamma = v/\Lambda$. Clearly this ratio cannot be too large as Λ_π is already bounded from below by collider and electroweak precision data [2]; Tevatron data for contact interactions yields the constraints $\Lambda_\pi \gtrsim 300,\ 1500,\ 4500\,\mathrm{GeV}$ for $k/\overline{M}_{Pl} = 1.0,\ 0.1,\ 0.01$, respectively. Curvature constraints suggest that $k/\overline{M}_{Pl} \leq 0.1$ [2], which in turn implies $v/\Lambda \lesssim 0.1$. For definiteness we will relax this bound somewhat and take $v/\Lambda \leq 0.2$ along with a physical Higgs mass of 125 GeV in our analysis. We note that large absolute values of ξ and wide ranges of v/Λ have been entertained in the literature.

The values of the two physical masses themselves are not arbitrary. When we require the weak eigenstate mass-squared parameters of the unmixed radion and Higgs fields to be real, as is demanded by hermiticity, we obtain an additional constraint on the ratio of the physical radion and Higgs masses which depends on both ξ and γ. Defining the ratio $r = (m_+/m_-)^2$, one finds that these two conditions require that r must be bounded from below by

$$r_{\min} = 1 + 2t^2 \pm 2|t|\sqrt{1+t^2}\,, \tag{9}$$

where the sign depends on the ordering of m_h and m_r. Note that this bound implies that it is disfavored for the radion to have a mass near that of the Higgs when there is significant mixing. The resulting excluded region is shown in figure 1 for the demonstrative case of $m_h = 125\,\mathrm{GeV}$. These constraints are found to be somewhat restrictive. The low mass region for the radion is also partially excluded by direct searches at LEP as can be seen from the figure. In calculating the LEP constraints, we fixed v/Λ to the conservative values of $v/\Lambda = 0.2(0.1)$ while varying ξ, and converted the LEP Higgs search bounds [8] into constraints for the radion using the appropriate set of rescaling factors. While some of the low mass region for the radion is eliminated for these values of the parameters, the parameter space for a light radion is certainly not closed. As one decreases the assumed fixed value of v/Λ, the size of the allowed low mass region grows since the radion couplings to the Z boson are rapidly shrinking.

JHEP08(2003)028

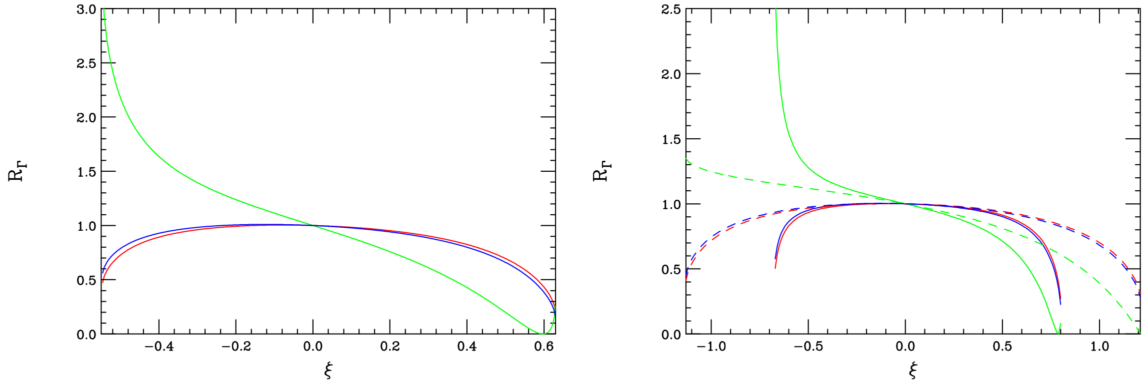

Figure 2: Ratio of Higgs partial widths to their SM values, R_Γ, as a function of ξ assuming a physical Higgs mass of 125 GeV: red for fermion pairs or massive gauge boson pairs, green for gluons and blue for photons. This corresponds to gluons, photons, $V\bar{V}$ from bottom to top on the right. In the top panel we assume $m_r = 300\,\mathrm{GeV}$ and $v/\Lambda = 0.2$. In the bottom panel the solid(dashed) curves are for $m_r = 500(300)\,\mathrm{GeV}$ and $v/\Lambda = 0.2(0.1)$.

Once ξ, γ and $m_{h,r}$ are specified, the angle θ describing the rotations into the Higgs-radion physical states becomes calculable; one finds that

$$\begin{aligned} \tan 2\theta &= \frac{2tZ^2 m_{h_0}^2}{m_{r_0}^2 - m_{h_0}^2(Z^2 - 36\xi^2\gamma^2)}\,, \\ \sin 2\theta &= \frac{2tm_{h_0}^2}{m_r^2 - m_h^2}\,. \end{aligned} \tag{10}$$

The weak basis masses are given by

$$m_{h_0}^2 = \frac{m_+^2 + m_-^2 \pm \sqrt{(m_+^2 + m_-^2)^2 - (2m_+m_-)^2(1+t^2)}}{2(1+t^2)}\,, \tag{11}$$

with the sign chosen positive(negative) when $m_h(m_r)$ is identified with $m_\pm$. In either case one obtains $m_{r_0} = Zm_+m_-/m_{h_0}$.

We now turn our attention to the properties of the Higgs boson in this model when mixing with the radion is included. Following the notation of Csaki et al. [7], the couplings of the physical Higgs to the SM fermions and massive gauge bosons $V = W, Z$ is now given by

$$\mathcal{L} = \frac{-1}{v}\left(m_f \bar{f} f - m_V^2 V_\mu V^\mu\right)\left[\cos\theta - t\sin\theta - \frac{v}{\Lambda}\frac{\sin\theta}{Z}\right] h\,, \tag{12}$$

where the angle θ is defined above and can now be calculated in terms of the four parameters ξ, v/Λ, and the physical Higgs and radion masses. Note that the shifts to the fermionic and massive gauge boson couplings are identical. Denoting the combinations $\alpha = \cos\theta - t\sin\theta$ and $\beta = -\sin\theta/Z$, the corresponding Higgs coupling to gluons can be written as

$$\mathcal{L} = c_g \frac{\alpha_s}{8\pi} G_{\mu\nu} G^{\mu\nu} h\,, \tag{13}$$

with

$$c_g = \frac{-1}{2v}\left[\left(\alpha + \frac{v}{\Lambda}\beta\right) F_g - 2b_3\beta\frac{v}{\Lambda}\right]. \tag{14}$$

JHEP08(2003)028

Here, the first term is the usual one-loop top-quark contribution to the ggh coupling, whereas the second term arises from the trace anomaly and appears solely from the mixing. $b_3 = 7$ is the SU(3) β-function and F_g is a well-known kinematic function of the ratio of masses of the top-quark to the physical Higgs boson [9]. Similarly the physical Higgs coupling to two photons is now given by

$$\mathcal{L} = c_\gamma \frac{\alpha_{em}}{8\pi} F_{\mu\nu} F^{\mu\nu} h \,, \tag{15}$$

where

$$c_\gamma = \frac{1}{v}\left[-\left(\alpha + \frac{v}{\Lambda}\beta\right) F_\gamma + (b_2 + b_Y)\beta\frac{v}{\Lambda}\right]. \tag{16}$$

Here, $b_2 = 19/6$ and $b_Y = -41/6$ are the SU(2) $\times$ U(1) β-functions and F_γ is another well-known kinematic function [9] of the ratios of the W boson and top-quark masses to the physical Higgs mass, and second term again originates from the trace anomaly. Note that in the simultaneous limits $\alpha \to 1$, $\beta \to 0$ we recover the usual SM results. From these expressions we can now compute the modifications to the various decay widths and branching fractions of the SM Higgs due to mixing with the radion.

Figure 2 shows the ratio of the various Higgs partial widths in comparison to their SM expectations as a function of the parameter ξ for sample values of m_r and v/Λ and assuming that $m_h = 125\,\mathrm{GeV}$. The range of the curves reflects the allowed parameter region for ξ. Several features are immediately apparent: (i) the shifts in the widths to $\bar{f}f/VV$ and $\gamma\gamma$ final states are very similar; this is due to the relatively large magnitude of F_γ while the combination $b_2 + b_Y$ is rather small. (ii) On the otherhand, the shift for the gg final state can be substantial; here, F_g is numerically smaller than F_γ and b_3 is quite large, resulting in a large contribution from the trace anomaly term. (iii) For relatively light radions with a lower value of Λ, the Higgs decay width into the gg final state can be vanishingly small. This is due to a strong destructive interference between the two contributions to the amplitude for values of ξ near -1. (iv) Increasing the value of m_r has less of an effect than does a decrease in the ratio v/Λ.

The deviation from SM expectations for the various branching fractions, as well as the total width, of the Higgs are displayed in figure 3 as a function of the mixing parameter ξ. As above, the range of the curves reflects the allowed parameter region for ξ. We see that the gluon branching fraction and the total width may be drastically different than that of the SM. As we will see below, the former may greatly affect the Higgs production cross section at the LHC. However, the $\gamma\gamma$, $f\bar{f}$, and VV (where $V = W, Z$) branching fractions only receive small corrections to their SM values, of order $\lesssim 5-10\%$ for almost all of the parameter region except near the edges of the parameter space. Observation of these shifts will require the precise determination of the Higgs branching fractions which is obtainable at a future high energy e^+e^- Linear Collider [10]. Once these measurements are performed, constraints on the radion parameter space may be extracted as will be discussed below. These small changes in the ZZh and $hb\bar{b}$ couplings of the Higgs boson can also lead to small reductions in the Higgs search reach from LEPII. This is presented in figure 4 for several sets of parameters; except for extreme parameter cases this reduction in reach is rather modest.

JHEP08(2003)028

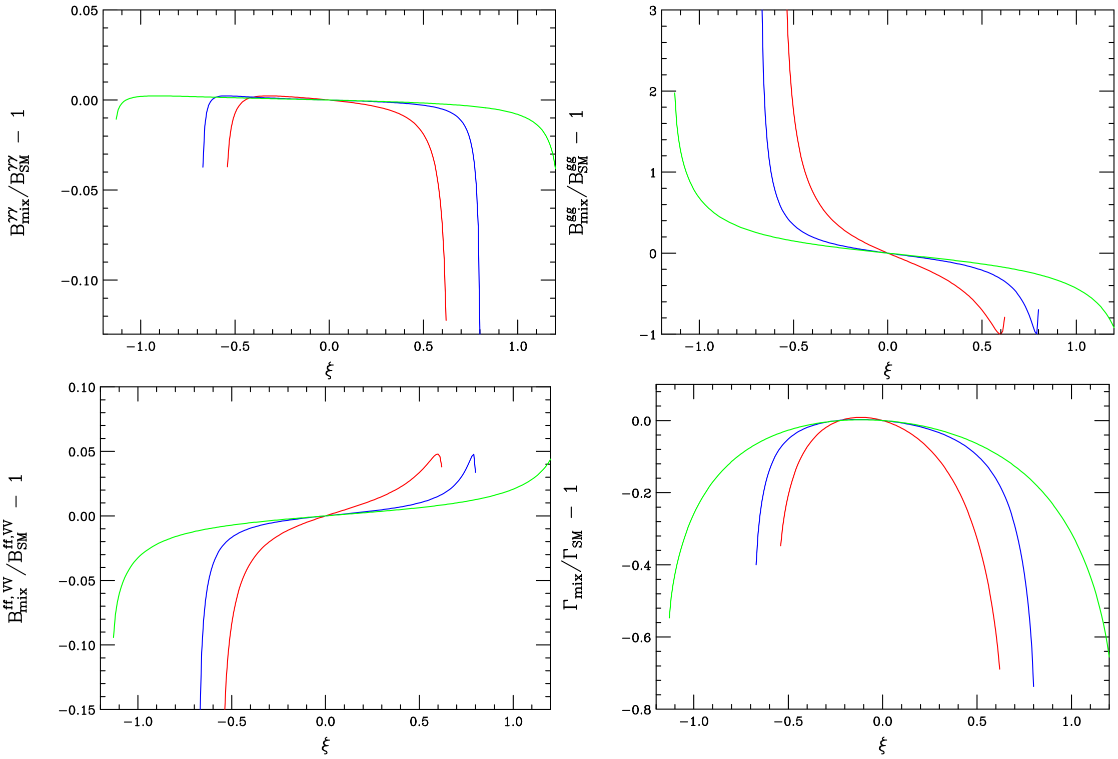

Figure 3: The ratio of the Higgs branching fraction into $\gamma\gamma$, gg, $f\bar{f}$, and VV final states as labeled, as well as for the total width, with radion mixing to that of the SM as a function of ξ. The red (blue; green) curves represent the choice $m_r = 300\,\mathrm{GeV}$, $v/\Lambda = 0.2$ (500, 0.2; 300, 0.1), and correspond to the curves which have the most limited (central; largest) range of ξ, respectively, in the figure.

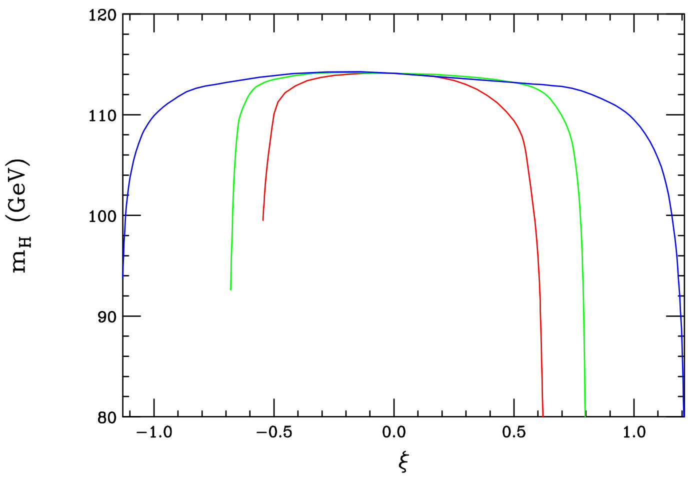

Figure 4: Lower bound on the mass of the Higgs boson from direct searches at LEP as a function of ξ including the effects of mixing. The red (green; blue) curves correspond to the choice $m_r = 300\,\mathrm{GeV}$, $v/\Lambda = 0.2$ (300, 0.1; 500, 0.2) and represent the curves from bottom to top.

At the LHC, the dominant production mechanism and signal for a light Higgs boson is gluon-gluon fusion through a triangle graph with subsequent decay into $\gamma\gamma$. Both the production cross section and the $\gamma\gamma$ branching fraction are modified by mixing with the

JHEP08(2003)028

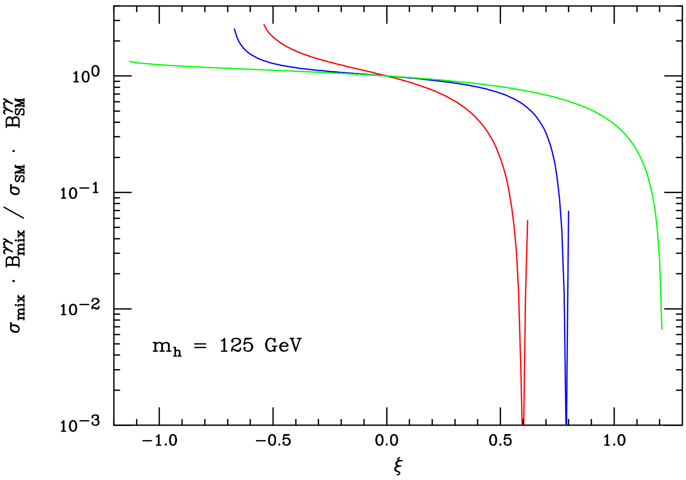

Figure 5: The ratio of production cross section times branching fraction for $pp \to h \to \gamma\gamma$ via gluon fusion with radion mixing to the SM expectations as a function of ξ. The Higgs mass is taken to be 125 GeV. The red (blue; green) curves correspond to the choice $m_r = 300\,\text{GeV}$, $v/\Lambda = 0.2$ (500, 0.2; 300, 0.1), from left to right on the r.h.s. of the figure.

radion, leading to the results illustrated in figure 5. This figure shows that the Higgs production rate in this channel at the LHC can be either significantly reduced or somewhat enhanced in comparison to the expectations of the SM due to the effects of mixing. For some values of the parameters the reduction can be by more than an order of magnitude which could seriously hinder the discovery of the Higgs via this channel at the LHC.

The s-channel production of the Higgs boson at a high energy photon photon collider is an important channel for determining the properties of the Higgs. In figure 6 we see that decreases in the production rate of the Higgs compared to SM expectations can also occur in the reaction $\gamma\gamma \to h \to b\bar{b}$ when mixing with the radion is included. Again, once such mixing is taken into account, the event rate is reduced, possibly hampering the statistical ability of a future high energy photon collider to measure the Higgs properties. However, note that the potential reductions in rate for this channel are not as drastic as those which may be realized at the LHC.

Once data from both the LHC and the Linear Collider (LC) is available, the radion parameter space can be explored using both direct searches and indirect measurements. In fact, the precision measurements of the Higgs boson couplings discussed above can be used to constrain the radion parameter space beyond what may be possible via direct searches for the radion. For purposes of demonstration, let us assume that the LHC and LC determine, within their capabilities, that the Higgs couplings are consistent with the predictions of the SM. Using the expectations for Higgs production at the LHC and LC from the analyses contained in ref. [10], we derive the resulting excluded regions in the $\xi - m_r$ parameter plane. This is displayed in figure 7 for various values of v/Λ for the sample case of $m_h = 125\,\text{GeV}$. In this figure, the allowed region lies between the corresponding pair of vertical curves. Here, we see that if such a set of measurements of the Higgs properties are realized, then a large fraction of the radion parameter space would be excluded. Direct radion searches

JHEP08(2003)028

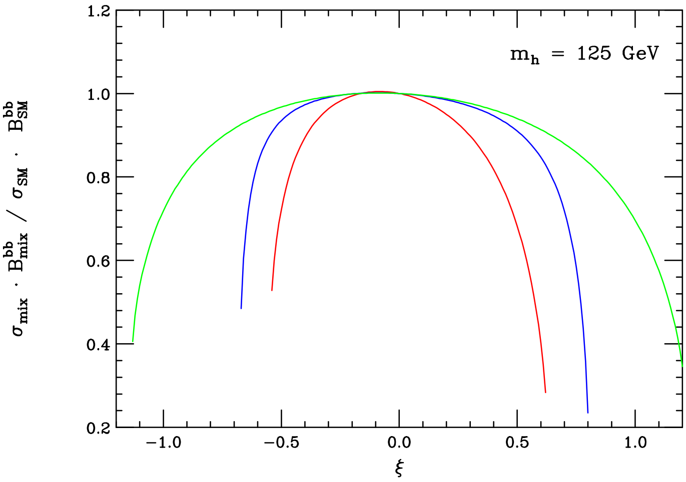

Figure 6: The ratio of production cross section times branching fraction for $\gamma\gamma \to h \to b\bar{b}$ with radion mixing to the SM expectations as a function of ξ. The Higgs mass is taken to be 125 GeV. The red (blue; green) curves, corresponding to the bottom (middle, top) curves, represent the parameter choices $m_r = 300\,\text{GeV}$, $v/\Lambda = 0.2$ (500, 0.2; 300, 0.1).

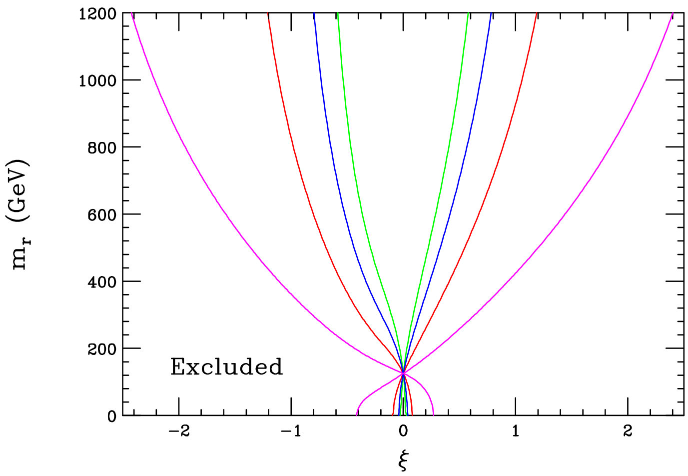

Figure 7: 95% CL indirect bounds on the mass and mixing of the radion arising from the precision measurements of the Higgs couplings obtainable at the LHC and a Linear Collider for a Higgs mass of 125 GeV. The allowed region lies between the corresponding pair of vertical curves. From the inner to outer curves, they represent the parameter values $v/\Lambda = 0.2, 0.15, 0.10$, and 0.05, respectively.

at these colliders would fully cover the lower portion of the remaining parameter space up to the radion search reach. Together, the direct and indirect constraints would then only allow for a high mass radion with small mixing as a possibility under this scenario.

Lastly, we note that the patterns of the shifts in the Higgs boson properties due to radion mixing are distinct from those in other models of new physics. For example, consider the two Higgs double model [9]. In this model, the ratio of the hVV coupling to its SM value is given by $\sin(\beta - \alpha)$ and the similar ratio for the $ht\bar{t}$ coupling is $\cos\alpha / \sin\beta$, where $\tan\beta$ is the ratio of vevs of the two Higgs doublets and α is the mixing angle between the two doublets. In one variant of this model, the corresponding ratio of the $hb\bar{b}$ coupling is equal, up to a sign, of that for the $ht\bar{t}$ coupling, while in a second version of the model the $hb\bar{b}$ ratio is $-\sin\alpha/\cos\beta$. In either case, this spectrum of couplings cannot be reproduced via radion mixing.

In summary, we see that Higgs-radion mixing, which is present in some extra dimensional scenarios, can have a substantial effect on the properties of the Higgs boson. These modifications affect the total and partial widths, as well as the branching fractions, of Higgs decay into various final states. This, in turn, can significantly alter the expectations for Higgs production at LEP, the LHC, and a photon collider. For some regions of the parameters, the size of these shifts in the Higgs widths and branching fractions may require the precision of a Linear Collider in order to be studied in detail.

Note added: a related paper [11] appeared on the arXiv four months after this work and one year after a preliminary version of this work was presented at summer conferences [12].

References

[1] L. Randall and R. Sundrum, *A large mass hierarchy from a small extra dimension*, *Phys. Rev. Lett.* **83** (1999) 3370 [hep-ph/9905221]; *An alternative to compactification*, *Phys. Rev. Lett.* **83** (1999) 4690 [hep-th/9906064].

[2] For an overview of RS phenomenology, see H. Davoudiasl, J.L. Hewett and T.G. Rizzo, *Phenomenology of the randall-sundrum gauge hierarchy model*, *Phys. Rev. Lett.* **84** (2000) 2080 [hep-ph/9909255];
H. Davoudiasl, J.L. Hewett and T.G. Rizzo, *The $(g-2)$ of the muon in localized gravity models*, *Phys. Lett.* **B 493** (2000) 135 [hep-ph/0006097]; *Experimental probes of localized gravity: on and off the wall*, *Phys. Rev.* **D 63** (2001) 075004 [hep-ph/0006041].

[3] W.D. Goldberger and M.B. Wise, *Modulus stabilization with bulk fields*, *Phys. Rev. Lett.* **83** (1999) 4922 [hep-ph/9907447]; *Phenomenology of a stabilized modulus*, *Phys. Lett.* **B 475** (2000) 275 [hep-ph/9911457];
C. Csáki, M. Graesser, L. Randall and J. Terning, *Cosmology of brane models with radion stabilization*, *Phys. Rev.* **D 62** (2000) 045015 [hep-ph/9911406];
C. Charmousis, R. Gregory and V.A. Rubakov, *Wave function of the radion in a brane world*, *Phys. Rev.* **D 62** (2000) 067505 [hep-th/9912160];
T. Tanaka and X. Montes, *Gravity in the brane-world for two-branes model with stabilized modulus*, *Nucl. Phys.* **B 582** (2000) 259 [hep-th/0001092].

[4] G.F. Giudice, R. Rattazzi and J.D. Wells, *Graviscalars from higher-dimensional metrics and curvature-Higgs mixing*, *Nucl. Phys.* **B 595** (2001) 250 [hep-ph/0002178].

[5] U. Mahanta and A. Datta, *Production of light stabilized radion at high energy hadron colliders*, *Phys. Lett.* **B 483** (2000) 196 [hep-ph/0002183];
T. Han, G.D. Kribs and B. McElrath, *Radion effects on unitarity in gauge-boson scattering*, *Phys. Rev.* **D 64** (2001) 076003 [hep-ph/0104074];
M. Chaichian, A. Datta, K. Huitu and Z.-h. Yu, *Radion and Higgs mixing at the LHC*, *Phys. Lett.* **B 524** (2002) 161 [hep-ph/0110035];
M. Chaichian, K. Huitu, A. Kobakhidze and Z.H. Yu, *Radions in a $\gamma\gamma$ collider*, *Phys. Lett.* **B 515** (2001) 65 [hep-ph/0106077];

S. Bae, P. Ko, H.S. Lee and J. Lee, *Phenomenology of the radion in the Randall-Sundrum scenario at colliders*, *Phys. Lett.* **B 487** (2000) 299 [hep-ph/0002224];
S. Bae and H.S. Lee, *Constraints on the radion from vacuum stability in the Randall-Sundrum theory*, *Phys. Lett.* **B 506** (2001) 147 [hep-ph/0011275];
S.C. Park, H.S. Song and J. Song, *Z boson pair production at LHC in a stabilized Randall-Sundrum scenario*, *Phys. Rev.* **D 65** (2002) 075008 [hep-ph/0103308];
S.R. Choudhury, A.S. Cornell and G.C. Joshi, *Radion signature in $\gamma\gamma$ scattering*, hep-ph/0012043;
K. Cheung, *Phenomenology of radion in Randall-Sundrum scenario*, *Phys. Rev.* **D 63** (2001) 056007 [hep-ph/0009232].

[6] G.D. Kribs, *Physics of the radion in the Randall-Sundrum scenario*, in *Proc. of the APS/DPF/DPB Summer Study on the Future of Particle Physics (Snowmass 2001)*, R. Davidson and C. Quigg eds., *eConf* **C010630** (2001) P317 [hep-ph/0110242].

[7] C. Csáki, M.L. Graesser and G.D. Kribs, *Radion dynamics and electroweak physics*, *Phys. Rev.* **D 63** (2001) 065002 [hep-th/0008151].

[8] For a recent summary of LEP Higgs boson searches and original references, see A. Sopczak, *Complete LEP data: status of Higgs boson searches*, *Phys. Atom. Nucl.* **65** (2002) 2116[hep-ph/0112082].

[9] J.F. Gunion, H.E. Haber, G.L. Kane and S. Dawson, *The Higgs hunter's guide,*, Addison-Wesley, Redwood City 1990.

[10] M. Battaglia and K. Desch, *Precision studies of the Higgs boson profile at the* e^+e^- *linear collider*, hep-ph/0101165;
See also, M. Carena, D.W. Gerdes, H.E. Haber, A.S. Turcot, and P.M. Zerwas, *Executive summary of the Snowmass 2001 working group on electroweak symmetry breaking*, in *Proc. of the APS/DPF/DPB Summer Study on the Future of Particle Physics*, R. Davidson and C. Quigg eds., hep-ph/0203229.

[11] D. Dominici, B. Grzadkowski, J.F. Gunion and M. Toharia, *The scalar sector of the Randall-Sundrum model*, hep-ph/0206192.

[12] J.L. Hewett and T.G. Rizzo, *Radion mixing effects on the properties of the standard model Higgs boson*, in *Proc. of the APS/DPF/DPB Summer Study on the Future of Particle Physics (Snowmass 2001)* N. Graf eds., *eConf* **C010630** (2001) P338 [hep-ph/0112343];
G. Azuelos et al., *The beyond the standard model working group: summary report*, in *Proceedings of Workshop on Physics at TeV Colliders*, Les Houches, France, 21 May - 1 Jun 2001, [hep-ph/0204031].

JHEP08(2003)028